

# 6-L-<sup>18</sup>F-Fluorodihydroxyphenylalanine PET in Neuroendocrine Tumors: Basic Aspects and Emerging Clinical Applications\*

Pieter L. Jager<sup>1</sup>, Raman Chirakal<sup>1</sup>, Christopher J. Marriott<sup>1</sup>, Adrienne H. Brouwers<sup>2</sup>, Klaas Pieter Koopmans<sup>2</sup>, and Karen Y. Gulenchyn<sup>1</sup>

<sup>1</sup>Department of Nuclear Medicine, Hamilton Health Sciences/McMaster University, Hamilton, Ontario, Canada; and <sup>2</sup>Department of Nuclear Medicine and Molecular Imaging, University Medical Center Groningen, Groningen, The Netherlands

In recent years, 6-L-<sup>18</sup>F-fluorodihydroxyphenylalanine (<sup>18</sup>F-DOPA) PET has emerged as a new diagnostic tool for the imaging of neuroendocrine tumors. This application is based on the unique property of neuroendocrine tumors to produce and secrete various substances, a process that requires the uptake of metabolic precursors, which leads to the uptake of <sup>18</sup>F-DOPA. This nonsystematic review first describes basic aspects of <sup>18</sup>F-DOPA imaging, including radiosynthesis, factors involved in tracer uptake, and various aspects of metabolism and imaging. Subsequently, this review provides an overview of current clinical applications in neuroendocrine tumors, including carcinoid tumors, pancreatic islet cell tumors, pheochromocytoma, paraganglioma, medullary thyroid cancer, hyperinsulinism, and various other clinical entities. The application of PET/CT in carcinoid tumors has unsurpassed sensitivity. In medullary thyroid cancer, pheochromocytoma, and hyperinsulinism, results are also excellent and contribute significantly to clinical management. In the remaining conditions, the initial experience with <sup>18</sup>F-DOPA PET indicates that it seems to be less valuable, but further study is required.

**Key Words:** <sup>18</sup>F-DOPA; PET; neuroendocrine tumors; carcinoid

**J Nucl Med 2008; 49:573–586**

DOI: 10.2967/jnumed.107.045708

**W**ith the growing expansion of <sup>18</sup>F-FDG PET in the functional imaging of cancer, the interest in other tracers has also grown. Although <sup>18</sup>F-FDG is unsurpassed for the imaging of most tumors, there are a few exceptions. Brain tumors are less suitable for <sup>18</sup>F-FDG PET because of the high

background in normal brain tissue. Radiolabeled amino acid imaging has partly filled this gap. Because the uptake of <sup>18</sup>F-FDG generally increases with tumor aggressiveness and growth rates, relatively indolent tumors, such as prostate cancer, are known to have generally poor <sup>18</sup>F-FDG uptake. In prostate cancer, imaging is further limited by urinary activity in the bladder. <sup>11</sup>C- or <sup>18</sup>F-labeled choline and analogs have been developed to overcome these problems (*1*).

Another tumor type with generally low uptake of <sup>18</sup>F-FDG is the group of neuroendocrine tumors. In recent years, 6-L-<sup>18</sup>F-fluorodihydroxyphenylalanine (<sup>18</sup>F-DOPA) has emerged as a metabolic tracer, allowing PET of these tumors. This application is based on the unique property of neuroendocrine tumors to produce and secrete a large variety of substances, a process that requires the uptake of metabolic precursors that potentially can be radiolabeled. Since the first publication on the application of <sup>18</sup>F-DOPA to imaging of the dopaminergic system in the striatum, numerous studies have been performed to study the applicability in patients with Parkinson's disease and related diseases (*2,3*). However, the application to the imaging of neuroendocrine tumors is relatively new.

The body of literature focusing on whole-body imaging with <sup>18</sup>F-DOPA PET in endocrine oncology is rapidly expanding and includes applications not only in various subgroups of endocrine cancers but also in benign neuroendocrine processes. Therefore, the aim of this review was to summarize current knowledge on the application of whole-body imaging with <sup>18</sup>F-DOPA PET in neuroendocrine tumors. For this purpose, we describe basic aspects, with lessons derived from neurologic applications, and currently available clinical data.

We performed a nonsystematic review of all publications on <sup>18</sup>F-DOPA PET in neuroendocrine tumors up to early May 2007. The publications reviewed in this article were found through a search of the PubMed MEDLINE database. This search strategy was complex and used combinations of terms, such as DOPA, F-DOPA, <sup>18</sup>F-DOPA, F18-DOPA,

Received Jul. 26, 2007; revision accepted Nov. 6, 2007.

For correspondence or reprints contact: Pieter L. Jager, MD, PhD, Department of Nuclear Medicine, Hamilton Health Sciences/McMaster University, 1200 Main St. West, Hamilton, Ontario L8N 3Z5, Canada.

E-mail: [jager@hhsc.ca](mailto:jager@hhsc.ca)

\*NOTE: FOR CE CREDIT, YOU CAN ACCESS THIS ACTIVITY THROUGH THE SNM WEB SITE ([http://www.snm.org/ce\\_online](http://www.snm.org/ce_online)) THROUGH APRIL 2009.

No potential conflict of interest relevant to this article was reported. This paper discusses investigational devices/drugs not yet approved by the FDA. COPYRIGHT © 2008 by the Society of Nuclear Medicine, Inc.

F18-fluorodopa, 6-fluoro-L-DOPA, and fluor(o)dihydroxyphenylalanine as identifiers for the tracer; PET, imaging, positron emission tomography, and radionuclide imaging as identifiers for the imaging method; and carcinoid, endocrine, neuroendocrine, gastroenteropancreatic, medullary thyroid, paraganglioma, and more as identifiers for tumor types and subtypes. Publications on other but similar tracers, such as  $^{11}\text{C}$ -labeled DOPA analogs or  $^{18}\text{F}$ -dopamine, were studied but were not included in the tables. Only articles published in the English language were included. Relevant case reports were also acceptable. Articles on Parkinson's disease or related neurologic diseases were excluded by using appropriate search terms. The reference lists of all articles were checked for unknown publications. Review papers without original data were excluded. We selected the most recent publications in situations in which the same group had published more than one article over time and in which it was highly likely that patient groups had overlapped. As close followers of the developments in this field over the last few years, we believe that this search was complete, to the best of our knowledge.

The full texts of the articles were reviewed, and we tried to extract and tabulate sensitivity or specificity values as far as was reasonably feasible. Other important aspects of the articles were recorded and are discussed.

## BASIC ASPECTS

Dihydroxyphenylalanine (DOPA) is an amino acid containing 2 hydroxyl groups on the phenol ring (Fig. 1). It can be radiolabeled with  $^{18}\text{F}$  in various locations in the molecule. In this review, we focus on DOPA radiolabeled in the 6 position only, 6-L- $^{18}\text{F}$ -fluorodihydroxyphenylalanine ( $^{18}\text{F}$ -DOPA), because this is the compound that is clinically used.

DOPA is an intermediate in the catecholamine synthesis pathway (Fig. 2). In this pathway, DOPA is produced after hydroxylation of the amino acid tyrosine, which may enter the cell from outside. DOPA may also be derived from phenylalanine, another essential amino acid. DOPA can be decarboxylated to dopamine by amino acid decarboxylase (AADC). It can also be converted by catechol-*O*-methyltransferase to 3,4-dihydroxyphenylacetic acid. The affinity of radioactive  $^{18}\text{F}$ -DOPA for catechol-*O*-methyltransferase metabolism appears to be low compared with the affinity for AADC conversion (4). The resulting products can both be processed further downstream in the catecholamine pathway. Intermediates formed in this pathway are also involved in the biosynthesis of melanin; therefore,  $^{18}\text{F}$ -DOPA and analogs have also been applied in melanoma imaging.

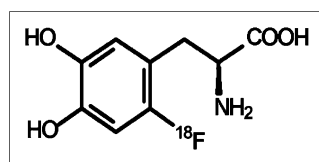


**FIGURE 1.** Chemical structure of  $^{18}\text{F}$ -DOPA.

## Radiosynthesis

Since the initial report on the application of  $^{18}\text{F}$ -DOPA to the assessment of presynaptic dopaminergic function in the human brain by PET, several methods have been published for the radiosynthesis of  $^{18}\text{F}$ -DOPA (2,5,6).  $^{18}\text{F}$ -labeled 6-fluoro-DOPA can be produced by either nucleophilic fluorination or electrophilic fluorination.

The nucleophilic method has the advantage that no-carrier-added  $^{18}\text{F}$ -fluoride is readily available in gigabecquerel quantities. However, the synthesis itself is a time-consuming, multistep procedure.

Regioselective electrophilic fluorination with  $^{18}\text{F}$ - $\text{F}_2$  or  $^{18}\text{F}$ -acetylhyperfluorite is done through fluorodemetalation reactions. In these reactions, regioselectivity is achieved by prior functionalization of the aromatic ring followed by fluorination. In all cases, the  $^{18}\text{F}$ -labeled intermediate is hydrolyzed by acid catalysis, and the final product is isolated by high-performance liquid chromatography. The fluorodemetalation reaction is successful because the carbon–metal bond is weaker than the carbon–hydrogen bond. As such, electrophilic attack is regioselective, with relatively high radiochemical yields. Organic derivatives of silicon, tin, and mercury have been used for the synthesis of  $^{18}\text{F}$ -DOPA. A remote, semiautomated method for fluorodemercuration and a fully automated “one-pot” synthesis method for fluorodestannylation were reported (7,8). Decay-corrected radiochemical yields were 11% and 35%, respectively, on the basis of the total amount of  $^{18}\text{F}$ - $\text{F}_2$  collected from the target. At present, regioselective fluorodestannylation is the most commonly used method for the routine production of  $^{18}\text{F}$ -6-fluorodopa.

Direct fluorination of fully protected DOPA with  $^{18}\text{F}$ -acetylhyperfluorite, followed by deprotection and high-performance liquid chromatography purification, is a good alternative for fluorodestannylation (6). The radiochemical yield (8%) is sufficient to produce useful quantities of  $^{18}\text{F}$ -DOPA for PET in humans. The original and simplest of all electrophilic fluorinating agents is fluorine gas. It has been shown that the reactivity of  $\text{F}_2$  toward organic compounds can be moderated by diluting it with an inert gas (9).  $^{18}\text{F}$ - $\text{F}_2$  is produced from a gas target containing 0.01%–0.2%  $\text{F}_2$  in neon (10–12). It has been shown that anhydrous hydrogen fluoride (aHF) or  $\text{BF}_3\cdot\text{aHF}$  is an ideal solvent for the low-temperature radiofluorination of DOPA, producing a mixture of  $^{18}\text{F}$ -labeled 2-fluorodopa, 5-fluorodopa, and 6-fluorodopa (13). During a typical production run,  $700 \pm 75$  MBq ( $18 \pm 2$  mCi) (mean  $\pm$  SD) of 6- $^{18}\text{F}$ -fluorodopa can be produced from 5.5 GBq (150 mCi) of  $^{18}\text{F}$ - $\text{F}_2$  over 60 min of synthesis time (13). However, this method is not desirable for automation and routine production because of the hazardous nature of aHF and the specialized fluoroplastic equipment and expertise required for its handling. Recently, it was demonstrated that the reactivity and selectivity of  $\text{F}_2$  toward DOPA in trifluoromethanesulfonic acid ( $\text{CF}_3\text{SO}_3\text{H}$ ) were comparable to those in aHF. Radiofluorination of DOPA in  $\text{CF}_3\text{SO}_3\text{H}$  resulted in the production of 2-fluorodopa and

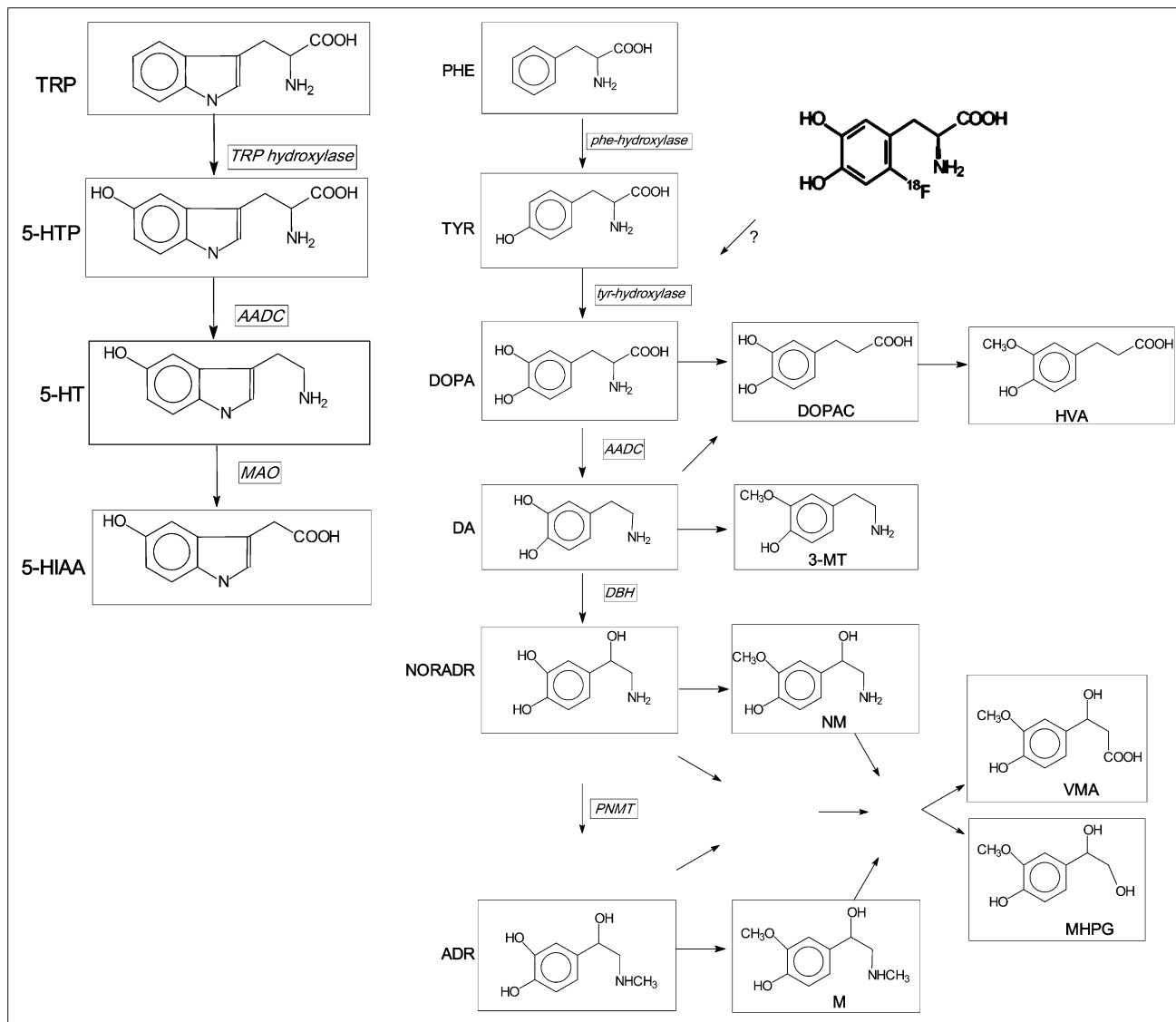


**FIGURE 2.** Catecholamine and serotonin synthesis pathways. ADR = adrenaline; DA = dopamine; DBH = dopamine- $\beta$ -hydroxylase; DOPAC = 3,4-dihydroxyphenylacetic acid; 5-HIAA = 5-hydroxyindolacetic acid; 5-HT = 5-hydroxytryptamine (serotonin); 5-HTP = 5-hydroxytryptophan; HVA = homovanillic acid; M = metanephrine; MAO = monoamine oxidase; MHPG = 3-methoxy-4-hydroxyphenylethylene glycol; 3-MT = 3-methoxytyramine; NM = normetanephrine; NORADR = noradrenaline; PHE = phenylalanine; PNMT = phenylethanolamine *N*-methyltransferase; TRP = tryptophan; TYR = tyrosine; VMA = vanillylmandelic acid.

6-fluorodopa at a radiochemical (decay-corrected) yield of  $17\% \pm 2\%$  over 55 min of synthesis time (14).

#### Intracellular Factors Involved in Tumor Uptake

The special property of neuroendocrine cells that distinguishes them from other cells includes the uptake and decarboxylation of monoamine precursors and the secretion of a large variety of products, of which serotonin is the most prominent. However, these cells may also produce other biogenic amines, such as catecholamine and histamine (15,16). Serotonin is produced after decarboxylation by AADC of the substrate 5-hydroxytryptophan, which is derived from plasma or from the intracellular hydroxylation of

tryptophan, another essential amino acid. This process of uptake of amine precursors is described in the amine precursor uptake and decarboxylation concept (17). The enzyme AADC is strongly expressed in neuroendocrine cells, and its activity plays a key role in this concept.

Like other tyrosine-based tracers, such as  $^{11}\text{C}$ -tyrosine,  $^{18}\text{F}$ -ethyltyrosine,  $^{123}\text{I}$ -methyltyrosine, and other analogs,  $^{18}\text{F}$ -DOPA enters cells through the amino acid transport systems for large neutral amino acids, which are present in nearly all cells (18–21). This process has been validated by blocking experiments with the neuroendocrine tumor cell line BON, in which the model substrate 2-amino-bicyclo-(2,2,1)-heptane-2-carboxylic acid (BCH) nearly

completely shuts down the cellular uptake of  $^{18}\text{F}$ -DOPA (22).

The fate of the tracer further downstream in the catecholamine pathway is less clear. Metabolites such as  $^{18}\text{F}$ -dopamine may subsequently enter intracellular storage vesicles present in some, but not all, neuroendocrine cells through transport mechanisms such as the vesicular monoamine transporter; in this way, they are effectively trapped inside the cell, at least for the time during which the radioactivity has not decayed. In cells lacking vesicular storage systems, the fate of  $^{18}\text{F}$ -DOPA is less clear.

Although transmembrane transport is directly responsible for the high uptake of  $^{18}\text{F}$ -DOPA in neuroendocrine tumor cells, there may be more mechanisms governing uptake. It is evident that cells producing serotonin or catecholamine have strongly upregulated their amino acid transporters to cover the increased demand for precursors in their overactive metabolic pathways. This process then leads to the high uptake of  $^{18}\text{F}$ -DOPA. However, amino acid tracers using the same transmembrane transport system, such as  $^{11}\text{C}$ -methionine,  $^{11}\text{C}$ -tyrosine, and  $^{123}\text{I}$ -methyltyrosine, do not localize to a great extent in neuroendocrine tumor cells (21). This finding indicates that the increased transmembrane transport of large amino acids by itself is not the only factor that governs uptake; similar to the behavior in striatal and brain tissue (as described later) and similar to observations made with  $^{11}\text{C}$ -labeled DOPA, AADC activity must play an essential role (23,24). It is possible that only tracers with a high affinity for AADC and whose metabolic products can subsequently be stored in intracellular vesicles remain in cells. Other tracers may enter but may also rapidly leave cells again. More experimental work clearly needs to be done to clarify these issues.

#### Extracellular Factors Involved in Tumor Uptake

Besides the intracellular mechanisms that are involved in the conversion and metabolization of  $^{18}\text{F}$ -DOPA, extracellular factors are also involved in the uptake of this tracer in neuroendocrine cells. However, most current knowledge is derived from striatal imaging in Parkinson's disease and related diseases.

After intravenous injection,  $^{18}\text{F}$ -DOPA is metabolized by the AADC enzyme activity present in many tissues, including the liver and especially the kidneys. Radiolabeled metabolites include 3-*O*-methyl- $^{18}\text{F}$ -DOPA, 6- $^{18}\text{F}$ -fluorodopamine, L-3,4-dihydroxy-6- $^{18}\text{F}$ -fluorophenylacetic acid, and 8- $^{18}\text{F}$ -fluorohomovanillic acid (25). In rat brain sections, the storage of  $^{18}\text{F}$ -dopamine in vesicles seemed to occur rapidly (25). Studies of brain imaging have demonstrated that many metabolites enter the striatum, cortex, and cerebellum to various degrees (26,27). Together with locally formed metabolites, up to 39%, 73%, and 80% of the tissue radioactivity at 30–90 min after injection was actually in the form of 3-*O*-methyl- $^{18}\text{F}$ -DOPA in the striatum, cortex, and cerebellum, respectively (28,29). In this respect, 3-*O*-methyl- $^{18}\text{F}$ -DOPA activity in the brain interferes with striatal assess-

ment. However, an initial rapid formation of  $^{18}\text{F}$ -dopamine at early time points after injection appears to decrease over time (29).

AADC was proven to be the driving force for the increased striatal uptake in many studies (29). Another interesting example of this mechanism was the observation of low to minimal  $^{18}\text{F}$ -DOPA uptake in an infant with an inborn deficiency of AADC (30).

#### Carbidopa

Carbidopa is routinely used in  $^{18}\text{F}$ -DOPA imaging in neurology, because it increases striatal uptake, mainly by increasing the concentration in plasma and decreasing renal excretion (31,32). Studying the effects of carbidopa in neuroendocrine tumors, Orlefors et al. (33) performed PET with  $^{11}\text{C}$ -5-hydroxytryptophan before and after carbidopa administration in 6 patients. Although the results may not be fully valid for  $^{18}\text{F}$ -DOPA, there were strong similarities in clinical behavior, uptake levels, and uptake mechanisms between these 2 tracers; these findings make that study relevant to  $^{18}\text{F}$ -DOPA PET as well. Carbidopa greatly reduced the high levels of uptake present in the renal pelvis and kidneys, by an average factor of 4 (range, 2–20) (33). Liver uptake increased slightly, and pancreatic uptake decreased considerably. The background uptake of  $^{11}\text{C}$ -5-hydroxytryptophan without carbidopa, however, appeared to be considerably higher than  $^{18}\text{F}$ -DOPA uptake. Of interest, tumor uptake increased markedly, with standardized uptake values (SUVs) increasing 10%–30%. These effects clearly improved the overall image quality and led to the detection of more lesions of carcinoid tumors (33). Similar studies with pheochromocytoma are currently being performed.

#### Image Acquisition

Whole-body imaging is usually performed in a manner similar to that of  $^{18}\text{F}$ -FDG PET, from the upper legs through the level of the skull, because lesions outside this area are infrequently observed. Many centers have used a 90-min interval between injection and imaging, but shorter intervals, of as little as 30 min, result in similar image quality. The required dose of activity varies largely and depends heavily on the camera, the acquisition protocols, availability, and costs. Fixed doses of as low as 100 MBq have resulted in adequate imaging. High doses, such as 5 MBq/kg of body weight, have also been applied. The tracer should be injected slowly, to avoid pharmacologic effects, which might induce a carcinoid crisis, especially when specific activity is low (34). At present, most studies are performed with PET/CT scanners. The radiation dose in  $^{18}\text{F}$ -DOPA PET is estimated to be about 0.02 mSv/MBq (32).

#### Appearance of Normal Whole-Body $^{18}\text{F}$ -DOPA PET Scan and Pitfalls

The normal appearance includes high uptake in the urinary excretion systems, including the collecting systems in the kidneys, ureters, and bladder (Fig. 3). High focal uptake in



**FIGURE 3.** Normal  $^{18}\text{F}$ -DOPA PET projection image with carbidopa pretreatment, showing major uptake in kidneys, ureter, and bladder and minor uptake in striatum, myocardium, liver, and muscles.

the gallbladder region and, in some cases, the common bile duct and focal uptake in the ureters may be misinterpreted as tumor uptake and requires careful comparison with CT or ultrasound in equivocal cases, in which tumor lesions may be present in the same region (35,36). Intermediate or low uptake levels are found in the striatum, myocardium, and liver. In general, low-level uptake can be observed in the small intestine and peripheral muscles. In children, some uptake in the growth plates can be seen. In other tissues,  $^{18}\text{F}$ -DOPA has minimal uptake and therefore provides good contrast against tumors. Uptake in the pancreas is of special interest, because it is nearly completely blocked after carbidopa administration. The precise reason for this finding is currently unclear. It may be based on the lack of vesicular storage vesicles in endocrine and exocrine pancreatic tissues in combination with the high level of competitive inhibition induced by carbidopa. This situation would lead to rapid pancreatic uptake and rapid efflux. These effects, however, have not been observed in dynamic imaging.

Of special note—and relevant for the detection of pheochromocytoma—is the minimal uptake in the normal adrenal medulla, the site of normal catecholamine synthesis. If  $^{18}\text{F}$ -DOPA were indeed a precursor in this pathway, then one would expect more uptake here. It is possible that this finding is the result of insufficient spatial resolution.

## CLINICAL RESULTS

### Carcinoid Tumors

Carcinoid tumors are relatively indolent tumors arising from neuroendocrine cells. They can produce and secrete a large variety of products because of their intrinsic ability to take up, accumulate, and decarboxylate amine precursors (17). Treatment options for carcinoid tumors include curative or debulking surgery, radiopeptide therapy, and medical treatment with somatostatin analogs and interferon (37–

39). For assessment of individual treatment options, knowledge of tumor localization, biochemical activity, and the rate of progression is essential. The initial work-up for patients with carcinoid tumors consists of morphologic imaging with methods such as CT combined with functional whole-body imaging with somatostatin receptor scintigraphy (SRS) (38–40). However, CT and MRI of the abdomen have difficulties in characterizing lesions as tumor deposits and in correctly distinguishing tumors and mesenteric metastases from intestinal structures (41,42).

There are now several reports that have focused on the application of  $^{18}\text{F}$ -DOPA PET in carcinoid tumors; however, only 3 of these were conducted as prospective studies, and only 2 specifically included only patients with carcinoid tumors (Table 1). Most other studies were retrospective and were often performed with mixed populations. However, with these drawbacks aside, the cumulative number of patients described was approximately 120. Sensitivity values were presented at the level of individual patients, body regions, individual lesions or, specifically, for primary tumors, organ metastases, and lymph node metastases. Therefore, the numbers are difficult to compare. In addition, there is the problem of the optimal reference standard, which is always difficult when a new technique detects previously unknown lesions. Various authors have made different choices in this matter. However, in general, high sensitivity values, in the range of 65%–96%, have been reported for the detection of individual lesions, and most of the values were in the upper half of this range. Examples are presented in Figures 4 and 5. The most extensive study was performed by Koopmans et al., who analyzed data at the patient, region, and lesion levels and found sensitivity values of 100%, 95%, and 96%, respectively; they used a composite reference standard consisting of all available imaging, cytologic, and histologic data (35). Carbidopa premedication was routinely used. In that study,  $^{18}\text{F}$ -DOPA PET alone detected more positive body regions and lesions than the combination of CT and SRS. Other authors have found high but somewhat lower sensitivity values, findings that may be related to different choices in reference standard methods or the lack of carbidopa pretreatment. Most studies that have included mixed groups have suggested that within the various subgroups of neuroendocrine tumor types, the performance of  $^{18}\text{F}$ -DOPA PET is relatively best for carcinoid tumors in comparison with the other subtypes.

$^{18}\text{F}$ -DOPA PET appears to be emerging as an excellent new staging method for patients with carcinoid tumors. When PET/CT instrumentation is used, anatomic information and whole-body staging information are provided by a single diagnostic tool; this combination has the potential to become the sole method for the assessment of carcinoid tumors. Preliminary studies appear to confirm this notion.

What is the clinical problem in patients with carcinoid tumors that  $^{18}\text{F}$ -DOPA may help to solve? In other words, what would be the clinical impact? Most studies so far have focused on patients with a known carcinoid tumor, and often

**TABLE 1**  
Published Clinical Applications of <sup>18</sup>F-DOPA PET in Malignant Tumors

Authors	Year	Reference	Tumor type	No. of patients	Basis for sensitivity determination	Sensitivity (%)	No. of lesions, regions, or patients	Specificity (%)	Reference standard	Other findings including sensitivities
Hoegerle et al.	1999	43	Carcinoid	1	Patients	100	1		Comp (H, I, FU)	First patient in literature
Hoegerle et al.	2001	44	Carcinoid/prospective	17/17	All lesions	65	92		Comp (H, I, FU)	SRS 57%, <sup>18</sup> F-FDG PET 29%, CT/MRI 73%
					Primary tumors	88				SRS 50%, CT 25%
					Lymph nodes	87				SRS 57%, CT 62%
					Organ metastases	65				SRS 57%, CT 97%; PET was best for primary tumors and lymph nodes
Becherer et al.	2004	45	Mixed/all prospective	18/23	All regions	83	54	96	CT	SRS 58% [overall]
					Region: bone	100	12			30-min postinjection interval was similar to 90-min interval
					Region: lung	20	5			
					Region: mediastinum	100	7			
					Region: liver	82	16			
					Region: pancreas	67	3			
					Region: lymph nodes	91	11			
Koopmans et al.	2006	35	Carcinoid/prospective	53/53	All patients	100	53		Comp (H, I, FU)	SRS 92%, CT 87%
					All regions	95	122	100		SRS 66%, CT 57%
					All lesions	96	687			
					Lesions: mediastinum	95	39			
					Lesions: lung	55	11			
					Lesions: liver	97	360			
					Lesions: pancreas	100	3			
					Lesions: abdomen	96	208			
					Lesions: bone	97	61			
					Lesions: extremities	100	5			
Montravers et al.	2006	46	Mixed/retrospective	17/32	All patients	63	32		?	SRS 78%
					Carcinoid	93	15	75		Specificity was based on 4 patients; SRS 81%
					Noncarcinoid	25	12			SRS 75%
Ambrosini et al.	2007	47	Mixed/retrospective	13/?	Patients with negative SRS results				Not applicable	Impact on management in 11/13 patients
Hoegerle et al.	2002	48	Pheochromocytoma	14	All patients	100	17		MRI	MBIG 71%
Hoegerle et al.	2003	49	Paraganglioma	10	Patients	80	10		MRI	PET correctly detected 3 more tumors
					Lesions	73	15			
Brink et al.	2006	50	Paraganglioma	1	Patient		1			PET detected lesions after resection
Boedeker et al.	2005	51	Paraganglioma	10	Patients				Comp	No results presented; positive general statements
Hoegerle et al.	2001	52	Medullary thyroid carcinoma	11	All lesions	63	27		(H, I, FU)	<sup>18</sup> F-FDG PET 44%, SRS 52%, CT/MRI 91%; CT/MRI had low specificities for primary tumors 55% and for recurrences 57%. <sup>18</sup> F-DOPA PET was better; <sup>18</sup> F-DOPA PET was best for lymph node staging
Beuthien-Baumann et al.	2007	53	Medullary thyroid carcinoma	15	Patients	46	15		H (partially)	<sup>18</sup> F-FDG 46%; <sup>18</sup> F-DOPA and <sup>18</sup> F-FDG were complementary
Jacob et al.	2003	54	Small cell lung cancer	4	Lesions	37	11		<sup>18</sup> F-FDG, CT, bone scan	<sup>18</sup> F-FDG yielded higher SUVs and detected more lesions
Dimitrakopoulou-Strauss et al.	2001	55	Melanoma	11	Patients		64	22	CT, ultrasound	<sup>18</sup> F-FDG 84%; <sup>18</sup> F-FDG uptake was 1.5 times higher, although in 4 patients, <sup>18</sup> F-DOPA uptake was higher
Seshadri et al.	2006	56	Melanoma	1	Lesions					High uptake in 2 adrenal metastases, similar to <sup>18</sup> F-FDG uptake
Langs et al.	2006	57	Hyperparathyroidism	8	Patients	0	8		H	No <sup>18</sup> F-DOPA uptake
Talbot et al.	2005	58	Merkel cell carcinoma	5	Patients	2	2		I, FU	<sup>18</sup> F-DOPA uptake was lower than <sup>18</sup> F-FDG uptake

Comp = composite reference standard; H = histology; I = imaging; FU = follow-up.

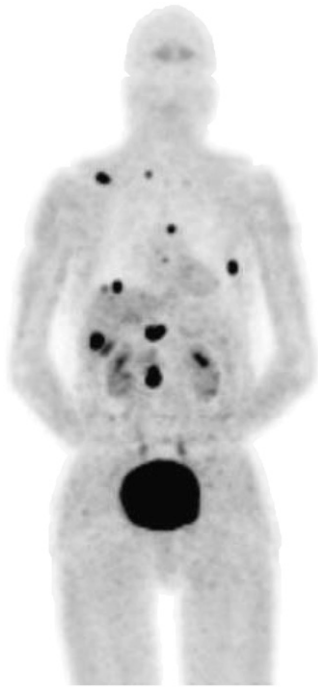


**FIGURE 4.**  $^{18}\text{F}$ -DOPA PET projection image with carbido-pa pretreatment in patient with carcinoid in several locations (abdomen, liver, mediastinum, and skeleton), confirming intense uptake and visualization even of very small lesions.

such patients had extensive metastatic disease. Although one could argue that it may not be useful to detect even more lesions than are already known, in daily practice the impact has been significant. Detection of extrahepatic disease may lead to cancellation of planned liver surgery or other debulking procedures, which are becoming more common for carcinoid tumors. Detection of disease metastatic to bone, which is often overlooked in carcinoid tumors, may have an impact on radiotherapy treatment. Determination of the amount and type of tumor burden has an impact on medical treatment choices. A better understanding of the tumor load in a patient may relate to prognosis, and patient organizations have reacted positively to these new diagnostic possibilities. From a diagnostic point of view,  $^{18}\text{F}$ -DOPA PET/CT might obviate SRS, which is relatively expensive, or other imaging modalities, thus simplifying and shortening the diagnostic process. In addition, the overall radiation dose may be decreased with the use of more specifically targeted diagnostic tools.

Although, in general,  $^{18}\text{F}$ -DOPA PET might replace SRS, there are situations in which SRS would still be mandatory.

This is the case in patients for whom radiopeptide treatment would be an option; an octreotide scan would still be required to study the uptake level and the feasibility of such treatment. However, in general, the relationship between metabolic information and somatostatin receptor expression is not clear. It is not a strict one-to-one relationship, because there are examples in which some tumor regions have apparently lost receptor expression while retaining  $^{18}\text{F}$ -DOPA avidity (Fig. 6). It will be intriguing to study the relationship between  $^{18}\text{F}$ -DOPA and PET-based variants of octreotide, such as  $^{68}\text{Ga}$ -DOTA-NOC (tetraazacyclododecane-tetracetic acid, [1-NaI3]-octreotide), once these have become more generally available (59). These agents have also led to the detection of significantly more lesions. A comparison of 2 PET-based imaging studies will also be more meaningful than a comparison with SPECT-based octreotide scanning, with its inherent limitation of spatial resolution.

An issue that has not yet been systematically studied is assessment of the response to treatment. It is well known that effective treatment often does not result in a detectable volume decrease, although clinical and biochemical parameters may indicate an adequate response (60). Similar to the application of  $^{18}\text{F}$ -FDG PET as an adjunct in response assessment, the metabolic information provided by  $^{18}\text{F}$ -DOPA PET may help in determining the results of treatment with, for example, existing or new drug regimens or radiotherapeutic or radiopeptide regimens.

Besides data for applications in patients with metastatic disease, few data are currently available on the application of  $^{18}\text{F}$ -DOPA PET in patients with only a suspected carcinoid tumor or similar neuroendocrine tumor, for example, patients with specific complaints and positive biochemistry results, such as increased chromogranin-A, 5-hydroxyindoleacetic acid, or catecholamine metabolite levels. It is predicted, and seems to be confirmed by clinical experience, that in this more difficult clinical situation, diagnostic accuracy parameters will be worse. Tumors may be too small to detect in such a situation. Although not explicitly published, the detection threshold will be on the order of a few millimeters, given the tremendous uptake of this tracer in carcinoid tissue.

Specificity, another important parameter, has not yet been established. To date, there have been no publications with clear false-positive findings, consistent with our clinical experience with several hundred cases. As with all diagnostic



**FIGURE 5.**  $^{18}\text{F}$ -DOPA PET (A), CT (B), and fused PET/CT (C) in patient with unusually large liver mass (thin arrows) with central necrosis, which was revealed to be carcinoid. PET also detected primary tumor (thick arrows) in lower left abdomen.

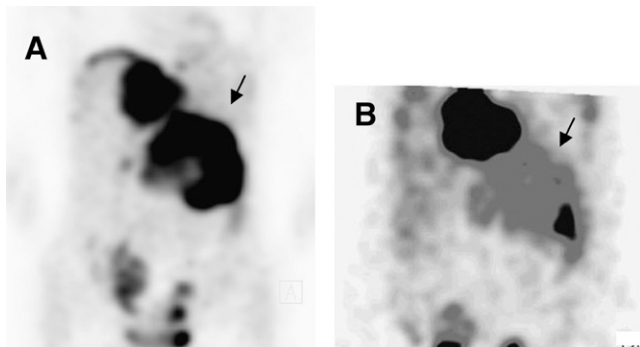


**FIGURE 6.**  $^{18}\text{F}$ -DOPA coronal view after carbidopa pretreatment in patient with metastasized carcinoid, showing heterogeneity of receptor expression and metabolic activity. (A)  $^{18}\text{F}$ -DOPA PET showing high uptake in entire process. (B) Considerably heterogeneous  $^{111}\text{In}$ -octreotide uptake. Apparently, medial part of this tumor (arrows) had lost most of its somatostatin receptor expression while retaining metabolic activity and  $^{18}\text{F}$ -DOPA uptake.

tools, there may be misinterpretations of borderline positive uptake versus background uptake. In addition, there have been cases in which a carcinoid tumor was accompanied by another tumor, with only the carcinoid tumor taking up  $^{18}\text{F}$ -DOPA and only the other (e.g., colorectal) tumor showing a positive  $^{18}\text{F}$ -FDG PET result.

Although theoretically a relationship between  $^{18}\text{F}$ -DOPA uptake and metabolic activity seems obvious, such a relationship has not been proven. Published evidence suggests the presence in both functioning and nonfunctioning tumors of uptake that is independent of the type of substance produced, for example, in both serotonin- and catecholamine-producing tumors (35). Diagnostic performance in foregut tumors, however, appears to be poorer than that in midgut tumors, a result that also suggests a relationship with metabolic activity.

In conclusion,  $^{18}\text{F}$ -DOPA PET has emerged as a new and exquisite new diagnostic tool for patients with carcinoid tumors; this tool adds important data for both clinicians and patients.

#### Pancreatic Islet Cell Tumors, Excluding Insulinoma

Islet cell tumors consist of different subtypes because they arise from various cells within the pancreas. The most common types are insulinoma (discussed later) and gastrinoma. Vasoactive intestinal peptide-secreting tumors, glucagonoma, and somatostatinoma are other, relatively less frequent subtypes. Carcinoid of the pancreas is rare. All of these tumors may exhibit malignant behavior and may dedifferentiate and metastasize. Up to 85% secrete biologically active products that may result in more or less specific clinical syndromes and that often aid in establishing the diagnosis.

Islet cell tumors can be very small. They nearly always express somatostatin receptors. Therefore, diagnostic imaging usually relies on morphologic imaging together with

SRS. Imaging is directed at finding the primary tumor for curative surgery whenever possible, but in the presence of metastatic disease, staging is necessary to determine the optimal treatment (such as chemotherapy, palliative surgery, radioablation, or observation) and to determine prognosis. An important imaging tool is endoscopic ultrasound (EUS), which may be able to detect tumors as small as 2–3 mm and which has sensitivity, specificity, and accuracy values of 82%, 95%, and 95%, respectively (61–63). Drawbacks are its operator dependency and the limited visualization of the pancreatic tail. MRI and especially CT have also shown generally good performance in detecting tumors as well as hepatic metastases, although the isodensity of pancreatic or hepatic lesions may limit applicability.

SRS and SPECT may identify many small tumors with adequate sensitivity, on the same order as or better than that of CT, MRI, or angiography. In addition, the acquisition of concomitant whole-body imaging helps in the assessment of extrapancreatic disease. However, for the frequently occurring hepatic metastases, CT and MRI may be more suitable.

$^{18}\text{F}$ -DOPA PET imaging appears to be less sensitive for these tumors than is SRS and to be less sensitive for these tumors than for carcinoid tumors, although in some cases it adds important staging information (Fig. 7). Although studies aimed specifically at this tumor type are lacking, they were included in nearly all studies focusing on mixed groups. The inferior results for these tumors relative to carcinoid tumors were consistently described in all of those studies (45–47).

#### Pheochromocytoma and Paraganglioma

Pheochromocytomas are rare catecholamine-producing neuroendocrine tumors arising from chromaffin cells of the adrenal medulla (in 80%–85% of cases) or from extraadrenal chromaffin tissues (in 15%–20% of cases), such as the paraganglia. They often produce typical clinical symptoms,

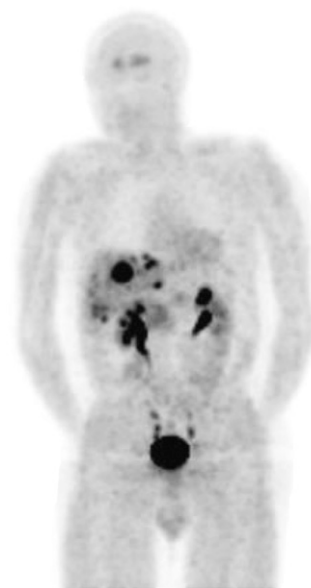


**FIGURE 7.**  $^{18}\text{F}$ -DOPA PET projection image with carbidopa pretreatment in patient with primary malignant islet cell tumor located in tail of pancreas and several liver metastases.

such as paroxysmal headaches, tachycardia, sweating, and hypertension. Malignant behavior can be found in 10%–20% of cases (64). The suggestion of a pheochromocytoma is usually based on these symptoms and increased catecholamine metabolite levels in urine or blood. Although this testing is quite sensitive, false-positive test results still occur; because of the rarity of this disease, they may exceed true-positive test results, especially when the increases in the levels of these metabolites are mild (64).

Besides biochemical testing, imaging of a suspected tumor contributes to arriving at a diagnosis and localizing the disease. CT and MRI have similar sensitivities for detecting the tumors, which are usually located in the adrenal glands; however, specificity is low (65). Scintigraphy with  $^{123}\text{I}$ -labeled metaiodobenzylguanidine (MIBG) is a very specific test (specificity, 95%–100%) and is frequently used to visualize pheochromocytomas, especially to search for extra-adrenal disease (66). Small pheochromocytomas, however, may be missed by MIBG scintigraphy, and in some (especially malignant) cases, the tumors do not take up MIBG.

In the head and neck region, paragangliomas may arise from similar neural crest cells and lead to the development of tumors at the carotid body, the jugular bulb, the tympanic plexus, and the vagus nerve. Patients frequently present with a painless neck mass. Biochemical activity is generally much less frequent in paragangliomas than in pheochromocytomas.

$^{18}\text{F}$ -DOPA PET has been used to a limited extent for pheochromocytomas. Hoegerle et al. found complete concordance between MRI and  $^{18}\text{F}$ -DOPA PET results in 17 patients, with significantly better performance of  $^{18}\text{F}$ -DOPA PET imaging than of MIBG imaging, which missed small tumors in 4 of 17 patients (48). The same group also found good results for paragangliomas of the head and neck region. MRI and PET results were concordant in 7 of 10 patients, showed partial agreement in 2 patients, and showed disagreement in 1 patient, in whom MRI could not confirm a lesion seen clearly on PET. All tumors diagnosed by MRI were found positive by PET; however, correlation of MRI and PET yielded an additional 3 lesions (49). A case report by Brink et al. confirmed the value of whole-body staging (50).

This finding was confirmed by our own experience (Fig. 8), but no additional original studies have been reported. In particular, uptake in malignant and metastatic lesions has not been confirmed.

Another PET tracer closely related to  $^{18}\text{F}$ -DOPA is  $^{18}\text{F}$ -fluorodopamine. It is currently unknown whether this radiopharmaceutical will be diagnostically superior or inferior to  $^{18}\text{F}$ -DOPA. Ilias et al. (67) and Pacak et al. (68) reported better sensitivity of  $^{18}\text{F}$ -fluorodopamine PET than of MIBG scanning, especially for malignant tumors.  $^{18}\text{F}$ -Fluorodopamine, however, is difficult to produce, and its specific activity is low. In addition, its uptake mechanism appears to be different, because it enters cells through the epinephrine transporter instead of a general amino acid transporter. In addition, it is in a more downstream position in the biochemical pathway, after AADC, and this position may result in different behaviors. Because paragangliomas usually express somatostatin receptors,  $^{68}\text{Ga}$ -based octreotide PET may be helpful in the work-up of patients with these tumors (69).

In conclusion, preliminary evidence indicates that  $^{18}\text{F}$ -DOPA PET could be a sensitive and specific tool for detecting pheochromocytomas, paragangliomas, and related tumors. It is probably more suitable than MIBG and may be used for whole-body staging, characterization of lesions, and early detection of tumors in patients who have SDHD mutations or von Hippel–Lindau disease and therefore are at increased risk.

#### Medullary Thyroid Cancer

Medullary thyroid cancer arises from the C cells in the thyroid and may be either sporadic or genetic in cases of multiple endocrine neoplasia, with rearrangement of the RET gene. Genetic testing now allows early detection and thyroidectomy at a young age. However, in many sporadic and older familial cases, calcitonin or carcinoembryonic antigen levels may rise shortly or many years after surgery, indicating residual or recurrent disease. Despite the use of many radiologic and nuclear medicine techniques to find the location of disease in such cases, detection remains difficult.

Attempts to use  $^{18}\text{F}$ -DOPA have produced reasonable results. Hoegerle et al. found an overall sensitivity of 63%

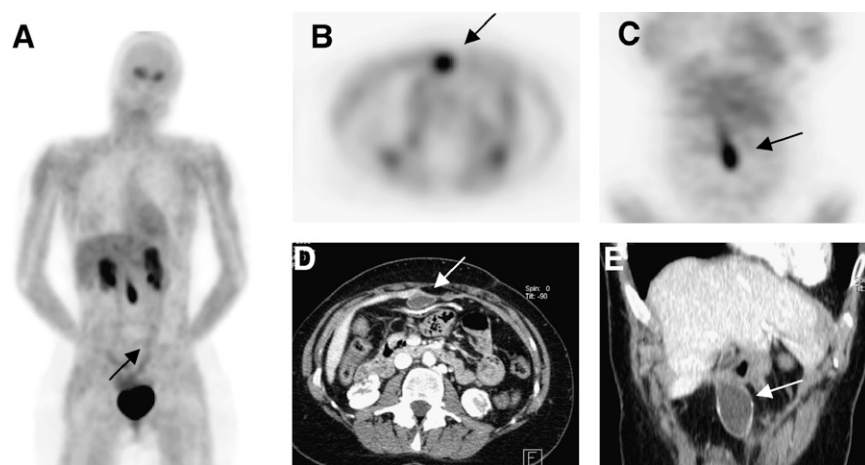


**FIGURE 8.**  $^{18}\text{F}$ -DOPA PET with CT, showing PET projection (A) and transverse PET (B), coronal PET (C), transverse CT (D), and coronal CT (E) views of patient with biochemical evidence of recurrent pheochromocytoma after previous adrenalectomy. Uptake can be seen in very ventrally located rounded lesion. Only after PET was combined with previously acquired CT (D and E) could this lesion (arrows) be clearly identified as site of recurrence.

for  $^{18}\text{F}$ -DOPA PET in 11 patients; this sensitivity was lower than that of CT/MRI but better than those of  $^{18}\text{F}$ -FDG PET and SRS (52). There may have been a bias toward the other modalities in that study, however, because only the findings of  $^{18}\text{F}$ -DOPA PET required histologic confirmation. In instances of discrepancies between CT/MRI and  $^{18}\text{F}$ -DOPA PET, PET correctly detected additional lesions in 6 patients. Reanalysis of these data appears to indicate that  $^{18}\text{F}$ -DOPA PET was superior to  $^{18}\text{F}$ -FDG in 4 of 11 cases, similar in 6 cases, and inferior in 1 case. PET was superior to SRS in 6 of 11 cases, similar in 3 of 11 cases, and inferior in 2 of 11 cases. In comparison with morphologic modalities,  $^{18}\text{F}$ -DOPA PET was superior in 3 of 11 cases, similar in 5 of 11 cases, and inferior in 3 of 11 cases. These data could lead to a preliminary conclusion that  $^{18}\text{F}$ -DOPA is a useful complementary tool for patients with medullary thyroid carcinoma.

In a retrospective analysis of  $^{18}\text{F}$ -DOPA PET in 15 patients with medullary thyroid carcinoma and increased levels of tumor markers, Beuthien-Baumann et al. found similar performances for  $^{18}\text{F}$ -FDG and  $^{18}\text{F}$ -DOPA; both yielded positive results in 7 of 15 patients, with lesions in the neck, mediastinum, abdomen, or bone (53). However, this was a retrospective study, with the problems inherent in such a study, and verification was available for only 2 patients. It is difficult to reach a conclusion from these findings, but they may suggest complementary roles for the 2 PET modalities. Interestingly, the authors observed minor adrenal uptake in 5 patients, which is not normally seen on  $^{18}\text{F}$ -DOPA PET. Preliminary findings from our own research suggested that  $^{18}\text{F}$ -DOPA PET was superior to  $^{18}\text{F}$ -FDG PET in patients with medullary thyroid carcinoma, especially when tumor marker progression rates were low. An example of our own experience is shown in Figure 9.

In conclusion, the limited available data suggest a potentially useful role for  $^{18}\text{F}$ -DOPA PET as a better or at least complementary modality that can add information to existing tests.

### Hyperinsulinism

Derived from the application of  $^{18}\text{F}$ -DOPA in general neuroendocrine tumors, this new PET method has also been applied in newborn babies with hyperinsulinism. This is a life-threatening, rather variable disease caused by dysregulation of insulin production, which may result in recurrent and persistent hypoglycemia, which in turn may lead to neurologic damage. Several, generally sporadic mutations in the genes encoding or regulating potassium channel proteins have been described as the underlying causes for this condition. Histologically, there are 2 subtypes, a focal form and a more diffuse form. Identification of the focal form is critical, as this subtype can be cured by limited partial pancreatectomy. In some children, however, medical therapy can be effective. Spontaneous regression has also been described. Current methods for identifying the focal subtype include complex and selective intrahepatic, intrapancreatic portal venous sampling. Other tests are arterial calcium stimulation

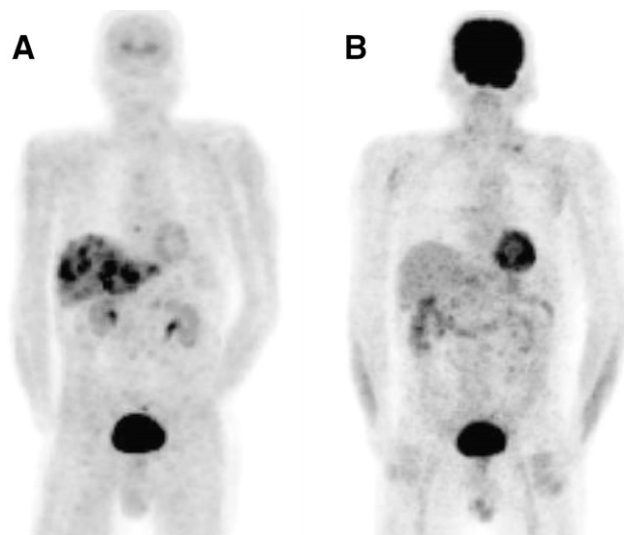


**FIGURE 9.**  $^{18}\text{F}$ -DOPA PET in patient with suspected recurrent medullary thyroid cancer, based on increased calcitonin level.  $^{18}\text{F}$ -DOPA PET (A) and  $^{18}\text{F}$ -FDG PET (B) showed clear  $^{18}\text{F}$ -DOPA uptake in liver metastases in absence of  $^{18}\text{F}$ -FDG uptake. Small area of  $^{18}\text{F}$ -FDG uptake in left supraclavicular region was result of nonspecific muscle activity.

and insulin response testing with venous sampling. Apart from being very complex, these tests require meticulous preparation of the baby and are far from perfect in accuracy. In some cases, blind 95% subtotal pancreatectomies are performed with the hope of curing the diffuse form of the disease, with acceptance of the high chance of inducing diabetes.

$^{18}\text{F}$ -DOPA PET has recently emerged as a new and promising modality for differentiating the histologic forms of this disease (Table 2). CT and MRI are generally less suitable, presumably because of the small size of the lesions and the similarity to normal tissue. There are now several articles describing the utility of  $^{18}\text{F}$ -DOPA PET for nearly 80 patients (Table 2), of which more than 50 underwent surgery. In 3 studies, the rate of prediction of the presence of the focal form by PET was 100% correct. In the largest study, by Hardy et al., there was one false-negative result, but sensitivity was still 96% (75). Because this is a very rare condition, investigators from several centers have proposed a standard protocol for performing the procedure (76). Medication (e.g., diazoxide, octreotide, and glucagon) should be discontinued for at least 2 d. Patients should fast for 6 h. A glucose infusion can be used to maintain euglycemia. The use of carbidopa is not recommended, because it may block both overall pancreatic uptake and uptake in the diseased area. Imaging should encompass at least the upper abdomen and middle abdomen and preferably be fused with CT. The distance between the pancreatic hilum and the “hot spot” is important to assist in surgical planning for tumors in the tail region of the pancreas. For interpretation, a ratio of the SUV for the suspected area to the mean for the entire pancreas of greater than 1.5 is strongly suggestive of disease.

A recent study focused on the localization of insulinomas in adult patients, which can also be quite difficult with

**TABLE 2**  
Published Clinical Applications of  $^{18}\text{F}$ -DOPA PET in Hyperinsulinism

Authors	Year	Reference	Disease type	Total no. of patients	No. of patients with indicated disease form		No. of patients undergoing surgery	No. (%) of patients for whom $^{18}\text{F}$ -DOPA PET results (vs. surgery) were correct	Other findings
					Focal	Diffuse			
Ribeiro et al.	2005	70	NHI	15	5	10	9 (5 with focal form + 4 with diffuse form)	9 (100)	
Otonkoski et al.	2006	71	NHI	14	5	9	9 (5 with focal form + 4 with diffuse form)	9 (100)	SUV of >50% for rest of pancreas
de Lonlay et al.	2006	72	NHI	7	3	4			ICH verification, patients from study of Ribeiro et al. (70)?
Kauhanen et al.	2007	73	Adult insulinoma	10	8	2	9	9 (100)	Sensitivity of PET (90%) was greater than those of CT (30%) and MRI (40%); in 50% of patients, PET results had impact on surgery
Hussain et al.	2006	74	NHI	1	1				PET detected focal ectopic lesion after unsuccessful earlier surgeries
Hardy et al.	2007	75	NHI	24	12	12	24	23 (96)	All focal lesions were correctly localized

NHI = neonatal hyperinsulinism; ICH = immunohistochemistry.

existing techniques, such as CT, EUS, MRI, or venous sampling (73). In the study of Kauhanen et al., in 10 patients with negative CT, EUS, or MRI results,  $^{18}\text{F}$ -DOPA PET localized a lesion in 9 patients, including 7 solid insulinomas, 1 malignant insulinoma, and 1 hepatic metastasis (73). These findings are in line with our own observations: both focal lesions and diffuse pancreatic uptake were noted in these patients. Diffuse uptake may be the result of nesidioblastosis, in which there is continued formation of new Langerhans' islands that produce insulin (Fig. 10).

Because all published studies have reported similar results and the conclusions of experts from different centers were uniformly positive, it seems safe to conclude that  $^{18}\text{F}$ -DOPA PET should be performed in all children affected by this condition and in whom surgery is being considered. In selected adult insulinomas, the method may also be useful, but more data are needed.

Although empirically clear, the driving force behind the relatively strong  $^{18}\text{F}$ -DOPA uptake in hyperinsulinistic tissue is less clear. Is it simply the increased amino acid transport activity induced by protein synthesis or insulin activity itself (77)? In that case, other radiolabeled amino acids should also be feasible.

#### Miscellaneous Conditions

**Small Cell Lung Cancer.** Because this tumor type may express neuroendocrine markers, Jacob et al. performed a very small study in 4 patients with small cell lung cancer and compared  $^{18}\text{F}$ -FDG and  $^{18}\text{F}$ -DOPA imaging (54). The performance of  $^{18}\text{F}$ -DOPA was relatively poor compared with that of  $^{18}\text{F}$ -FDG PET and conventional imaging, because

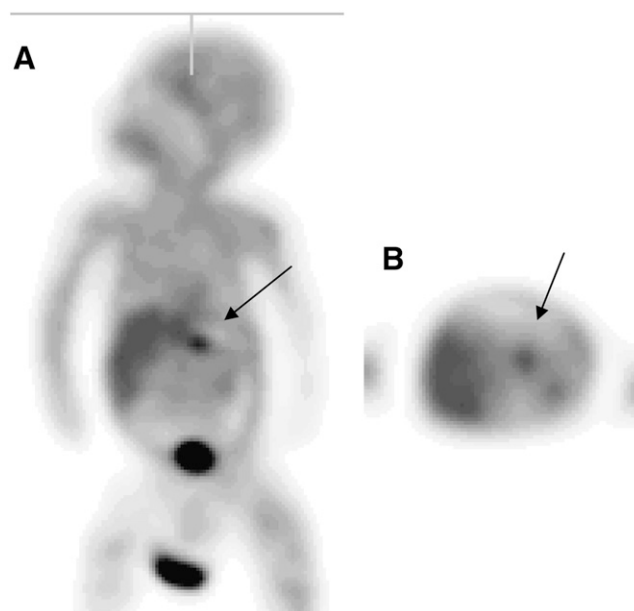


**FIGURE 10.**  $^{18}\text{F}$ -DOPA PET projection image (A) and transverse slice through pancreas (B) without carbidopa pretreatment in infant with congenital hyperinsulinism. PET suggested focal lesion (arrows) in body of pancreas, which was confirmed surgically.

$^{18}\text{F}$ -DOPA missed several lesions and the tumor uptake of  $^{18}\text{F}$ -DOPA (without carbidopa) was significantly lower than the uptake of  $^{18}\text{F}$ -FDG (median SUVs: 1.9 for  $^{18}\text{F}$ -DOPA and 5.9 for  $^{18}\text{F}$ -FDG). In their 4 patients, a relationship between neuroendocrine markers and  $^{18}\text{F}$ -DOPA uptake was absent. The authors suggested that  $^{18}\text{F}$ -DOPA uptake may reflect better differentiation of these tumors, but more data are required for this tumor type.

**Melanoma.** Dimitrakopoulou-Strauss et al. performed dynamic imaging in pretreated patients with melanomas and found a lesion-based sensitivity of 64% (14/22), whereas  $^{18}\text{F}$ -FDG detected 19 (86%) of the 22 lesions in 11 patients (55). In addition, the uptake of  $^{18}\text{F}$ -FDG was higher than the uptake of  $^{18}\text{F}$ -DOPA in 18 of 22 lesions, although in 4 liver lesions, the uptake of  $^{18}\text{F}$ -DOPA was higher. Seshadri et al. described a case in which avid uptake of both  $^{18}\text{F}$ -DOPA and  $^{18}\text{F}$ -FDG was noted in large bilateral adrenal melanoma metastases that were found negative by MIBG (56).

**Merkel Cell Tumors.** Talbot et al. found agreement among SRS,  $^{18}\text{F}$ -FDG PET, and  $^{18}\text{F}$ -DOPA PET in 3 patients (58). In 2 patients,  $^{18}\text{F}$ -FDG and  $^{18}\text{F}$ -DOPA appeared to be taken up by the tumor, although the tumor uptake of  $^{18}\text{F}$ -FDG was higher. In a case of recurrent Merkel cell tumor, SRS results were repeatedly positive, whereas  $^{18}\text{F}$ -DOPA PET results were negative and may have been correct.

**Hyperparathyroidism.** In none of 8 patients with surgically proven hyperparathyroidism,  $^{18}\text{F}$ -DOPA uptake was noted, whereas ultrasound or  $^{99\text{m}}\text{Tc}$ -MIBI imaging results were positive (57). Our own unpublished experience indicates similar findings, although with slightly better results, but basically there appears to be no added value of  $^{18}\text{F}$ -DOPA PET for this entity.

**Neuroblastoma.** On the basis of the good results of  $^{18}\text{F}$ -DOPA imaging for pheochromocytomas, it is predictable that results for neuroblastomas should also be good. No series have been published so far. In a single infant, however, with a suspected residual neuroblastoma that could not be localized by MRI, we performed  $^{18}\text{F}$ -DOPA PET and found a large retrovesical lesion that was difficult to recognize with MRI but proved to be residual disease.

**Brain Tumors.**  $^{18}\text{F}$ -DOPA PET has also been applied in brain tumors and performed better than  $^{18}\text{F}$ -FDG in demonstrating low-grade tumors and differentiating between recurrences and posttreatment scarring (78). However, this uptake was presumably based on the general amino acid nature of  $^{18}\text{F}$ -DOPA and not on its specific neuroendocrine tumor avidity.

**Difficult Clinical Cases.**  $^{18}\text{F}$ -DOPA PET is frequently used to study a large variety of unclear clinical conditions in which biochemical or clinical evidence indicates the presence of an endocrine disorder. Although there is no structured analysis of such cases available in current literature, many centers share this experience. An example is a case derived from our own experience, in a patient with severe Cushing's disease based on metastatic prostate cancer with neuroendocrine differentiation. All imaging had failed to identify the source of corticotropin overproduction; finally,  $^{18}\text{F}$ -DOPA

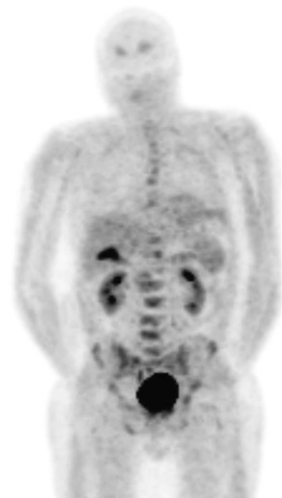


**FIGURE 11.**  $^{18}\text{F}$ -DOPA PET projection image in patient with Cushing's disease and in whom all imaging had failed to find source of corticotropin overproduction. PET showed significant bone marrow uptake, which proved to be metastatic prostate cancer with neuroendocrine differentiation after biopsy.

was performed and demonstrated diffuse uptake in the vertebral column. A subsequent biopsy demonstrated prostate cancer with neuroendocrine differentiation (Fig. 11).

## CONCLUSION

$^{18}\text{F}$ -DOPA PET is a new diagnostic tool for the imaging of various neuroendocrine tumors. This amino acid tracer is taken up through ubiquitous transmembrane amino acid transporter systems that are significantly upregulated in neuroendocrine tumors. This upregulation is presumably secondary to the increased activity of metabolic pathways involving the enzyme AADC, the key enzyme in substance secretion, which is a specific property of these tumors. Most experience exists in the field of carcinoid tumors, for which it has been demonstrated that  $^{18}\text{F}$ -DOPA PET has excellent sensitivity and detects significantly more disease than all other currently applied modalities, with a significant effect on patient management. In other conditions, such as medullary thyroid cancer, paraganglioma, and pheochromocytoma, experience is more limited, but current results suggest very good performance. In hyperinsulinic states, especially in newborns,  $^{18}\text{F}$ -DOPA PET has become the method of choice for differentiating between focal and diffuse pancreatic disease origins, with a direct impact on management. In pancreatic islet cells, results are less favorable and are similar to those obtained with currently used modalities. Very little information is available on application in hyperparathyroidism, small cell lung cancer, and melanoma, but these appear to be less favorable applications. Finally,  $^{18}\text{F}$ -DOPA PET, in general, frequently solves diagnostic problems in difficult clinical cases, which are frequently encountered in the work-up of proven and suspected neuroendocrine tumors.

## REFERENCES

1. Powles T, Murray I, Brock C, Oliver T, Avril N. Molecular positron emission tomography and PET/CT imaging in urological malignancies. *Eur Urol.* 2007;51:1511–1520.
2. Garnett ES, Firnau G, Nahmias C. Dopamine visualized in the basal ganglia of living man. *Nature.* 1983;305:137–138.

3. Fischman AJ. Role of [<sup>18</sup>F]-dopa-PET imaging in assessing movement disorders. *Radiol Clin North Am*. 2005;43:93–106.
4. Creveling CR, Kirk KL. The effect of ring-fluorination on the rate of O-methylation of dihydroxyphenylalanine (DOPA) by catechol-O-methyltransferase: significance in the development of <sup>18</sup>F-PET scanning agents. *Biochem Biophys Res Commun*. 1985;130:1123–1131.
5. Snyder SE, Kilbourn MR. Chemistry of fluorine-18 radiopharmaceuticals. In: Welch MJ, Redvanly CS, eds. *Handbook of Radiopharmaceuticals*. New York, NY: John Wiley & Sons Ltd.; 2003:195.
6. Luxen A, Guillaume M, Melega WP, Pike VW, Solin O, Wagner R. Production of 6-[<sup>18</sup>F]fluoro-L-DOPA and its metabolism in vivo: a critical review. *Nucl Med Biol*. 1992;19:149–158.
7. Luxen A, Perlmutter M, Bida GT, et al. Remote, semiautomated production of 6-[<sup>18</sup>F]fluoro-L-dopa for human studies with PET. *Int J Rad Appl Instrum [A]*. 1990;41:275–281.
8. De Vries EFJ, Luurtsema G, Brüßermann M, Elsinga PH, Vaalburg W. Fully automated synthesis module for the high yield one-pot preparation of 6-[<sup>18</sup>F]-fluoro-L-DOPA. *Appl Radiat Isot*. 1999;51:389–394.
9. Fukuhara N, Bigelow LA. The action of elementary fluorine upon organic compounds. XI. The vapor phase fluorination of benzene. *J Am Chem Soc*. 1941;63:2792–2795.
10. Casella V, Ido T, Wolf AP, Fowler JS, MacGregor RR, Ruth TJ. Anhydrous F-18 labeled elemental fluorine for radiopharmaceutical preparation. *J Nucl Med*. 1980;21:750–757.
11. Chirakal R, Adams RM, Firnao G, Schrobilgen GJ, Coates G, Garnett ES. Electrophilic <sup>18</sup>F from a Siemens 11 MeV proton-only cyclotron. *Nucl Med Biol*. 1995;22:111–116.
12. Nickles RJ, Daube ME, Ruth TJ. An <sup>18</sup>O target for the production of [<sup>18</sup>F]F2. *Appl Radiat Isot*. 1984;35:117–123.
13. Chirakal R, Firnao G, Garnett ES. High-yield synthesis of fluorodopa. *J Nucl Med*. 1986;27:417–421.
14. Behnam-Azad B, Chirakal RV, Schrobilgen GJ. Trifluoromethanesulfonic acid, an alternative solvent medium for the direct electrophilic fluorination of DOPA: new syntheses of 6-[<sup>18</sup>F]fluoro-L-DOPA and 6-[<sup>18</sup>F]fluoro-D-DOPA. *J Labelled Comp Radiopharm*. 2007;50:1236–1241.
15. Meijer WG, Copray SC, Hollma H, et al. Catecholamine-synthesizing enzymes in carcinoid tumors and pheochromocytomas. *Clin Chem*. 2003;49:586–593.
16. Kema IP, de Vries EG, Slooff MJ, Biesma B, Muskiet FA. Serotonin, catecholamines, histamine, and their metabolites in urine, platelets, and tumor tissue of patients with carcinoid tumors. *Clin Chem*. 1994;40:86–95.
17. Pearse AG. The APUD cell concept and its implications in pathology. *Pathol Annu*. 1974;9:27–41.
18. Heiss P, Mayer S, Herz M, Wester HJ, Schwaiger M, Senekowitsch-Schmidtke R. Investigation of transport mechanism and uptake kinetics of O-(2-[<sup>18</sup>F]fluoroethyl)-L-tyrosine in vitro and in vivo. *J Nucl Med*. 1999;40:1367–1373.
19. Lahoutte T, Cavelliers V, Camargo SM, et al. SPECT and PET amino acid tracer influx via system L (h4F2hc-hLAT1) and its transstimulation. *J Nucl Med*. 2004;45:1591–1596.
20. Jager PL, Vaalburg W, Pruim J, de Vries EG, Langen KJ, Piers DA. Radiolabeled amino acids: basic aspects and clinical applications in oncology. *J Nucl Med*. 2001;42:432–445.
21. Jager PL, Meijer WG, Kema IP, Willemse PH, Piers DA, de Vries EG. L-3-[<sup>123</sup>I]iodo- $\alpha$ -methyltyrosine scintigraphy in carcinoid tumors: correlation with biochemical activity and comparison with [<sup>111</sup>In-DTPA-D-Phe1]-octreotide imaging. *J Nucl Med*. 2000;41:1793–1800.
22. Neels OC, Jager PL, Koopmans KP, de Vries EGE, Kema IP, Elsinga PH. In vitro uptake studies in a neuroendocrine tumour cell line with PET [abstract]. *Eur J Nucl Med Mol Imaging*. 2006;33:427.
23. Bergström M, Eriksson B, Oberg K, et al. In vivo demonstration of enzyme activity in endocrine pancreatic tumors: decarboxylation of carbon-11-DOPA to carbon-11-dopamine. *J Nucl Med*. 1996;37:32–37.
24. Gilbert JA, Bates LA, Ames MM. Elevated aromatic-L-amino acid decarboxylase in human carcinoid tumors. *Biochem Pharmacol*. 1995;50:845–850.
25. Deep P, Gjedde A, Cumming P. On the accuracy of an [<sup>18</sup>F]FDOPA compartmental model: evidence for vesicular storage of [<sup>18</sup>F]fluorodopamine in vivo. *J Neurosci Methods*. 1997;76:157–165.
26. Leenders KL, Salmon EP, Tyrell P, et al. The nigrostriatal dopaminergic system assessed in vivo by positron emission tomography in healthy volunteer subjects and patients with Parkinson's disease. *Arch Neurol*. 1990;47:1290–1298.
27. Wahl L, Nahmias C. Modeling of fluorine-18-6-fluoro-L-Dopa in humans. *J Nucl Med*. 1996;37:432–437.
28. Melega WP, Grafton ST, Huang SC, Satyamurthy N, Phelps ME, Barrio JR. L-6-[<sup>18</sup>F]fluoro-dopa metabolism in monkeys and humans: biochemical parameters for the formulation of tracer kinetic models with positron emission tomography. *J Cereb Blood Flow Metab*. 1991;11:890–897.
29. Endres CJ, DeJesus OT, Uno H, Doudet DJ, Nickles JR, Holden JE. Time profile of cerebral [<sup>18</sup>F]6-fluoro-L-DOPA metabolites in nonhuman primate: implications for the kinetics of therapeutic L-DOPA. *Front Biosci*. 2004;9:505–512.
30. Hsieh HJ, Lin SH, Liu HM. Visualisation of impaired dopamine biosynthesis in a case of aromatic L-amino acid decarboxylase deficiency by co-registered <sup>18</sup>F-FDOPA PET and magnetic resonance imaging. *Eur J Nucl Med Mol Imaging*. 2005;32:517.
31. Hoffman JM, Melega WP, Hawk TC, et al. The effects of carbidopa administration on 6-[<sup>18</sup>F]fluoro-L-dopa kinetics in positron emission tomography. *J Nucl Med*. 1992;33:1472–1477.
32. Brown WD, Oakes TR, DeJesus OT, et al. Fluorine-18-fluoro-L-DOPA dosimetry with carbidopa pretreatment. *J Nucl Med*. 1998;39:1884–1891.
33. Orlefors H, Sundin A, Lu L, et al. Carbidopa pretreatment improves image interpretation and visualisation of carcinoid tumours with <sup>11</sup>C-5-hydroxytryptophan positron emission tomography. *Eur J Nucl Med Mol Imaging*. 2006;33:60–65.
34. Koopmans KP, Brouwers AH, De Hooge MN, et al. Carcinoid crisis after injection of 6-<sup>18</sup>F-fluorodihydroxyphenylalanine in a patient with metastatic carcinoid. *J Nucl Med*. 2005;46:1240–1243.
35. Koopmans KP, de Vries EG, Kema IP, et al. Staging of carcinoid tumours with <sup>18</sup>F-DOPA PET: a prospective, diagnostic accuracy study. *Lancet Oncol*. 2006;7:728–734.
36. Balan KK. Visualization of the gall bladder on F-18 FDOPA PET imaging: a potential pitfall. *Clin Nucl Med*. 2005;30:23–24.
37. Moertel CG. An odyssey in the land of small tumors. *J Clin Oncol*. 1987; 5:1503–1522.
38. Modlin IM, Latich I, Zikusoka M, Kidd M, Eick G, Chan AK. Gastrointestinal carcinoids: the evolution of diagnostic strategies. *J Clin Gastroenterol*. 2006;40: 572–582.
39. Plöckinger U, Rindi G, Arnold R, et al. Guidelines for the diagnosis and treatment of neuroendocrine gastrointestinal tumours: a consensus statement on behalf of the European Neuroendocrine Tumour Society (ENETS). *Neuroendocrinology*. 2004;80:394–424.
40. Oberg K. Neuroendocrine tumors of the gastrointestinal tract: recent advances in molecular genetics, diagnosis, and treatment. *Curr Opin Oncol*. 2005;17:386–391.
41. Kaltsas G, Rockall A, Papadogias D, et al. Recent advances in radiological and radionuclide imaging and therapy of neuroendocrine tumours. *Eur J Endocrinol*. 2004;151:15–27.
42. Rockall AG, Reznick RH. Imaging of neuroendocrine tumours (CT/MR/US). *Best Pract Res Clin Endocrinol Metab*. 2007;21:43–68.
43. Hoegerle S, Schneider B, Kraft A, Moser E, Nitzsche EU. Imaging of a metastatic gastrointestinal carcinoid by F-18-DOPA positron emission tomography. *Nuklearmedizin*. 1999;38:127–130.
44. Hoegerle S, Althoefer C, Ghanem N, et al. Whole-body <sup>18</sup>F dopa PET for detection of gastrointestinal carcinoid tumors. *Radiology*. 2001;220:373–380.
45. Becherer A, Szabó M, Karanikas G, et al. Imaging of advanced neuroendocrine tumors with <sup>18</sup>F-FDOPA PET. *J Nucl Med*. 2000;45:1161–1167.
46. Montravers F, Grahek D, Kerrou K, et al. Can fluorodihydroxyphenylalanine PET replace somatostatin receptor scintigraphy in patients with digestive endocrine tumors? *J Nucl Med*. 2006;47:1455–1462.
47. Ambrosini V, Tomassetti P, Rubello D, et al. Role of <sup>18</sup>F-dopa PET/CT imaging in the management of patients with <sup>111</sup>In-pentetreotide negative GEP tumours. *Nucl Med Commun*. 2007;28:473–477.
48. Hoegerle S, Nitzsche E, Althoefer C, et al. Pheochromocytomas: detection with <sup>18</sup>F DOPA whole body PET—initial results. *Radiology*. 2002;222:507–512.
49. Hoegerle S, Ghanem N, Althoefer C, et al. <sup>18</sup>F-DOPA positron emission tomography for the detection of glomus tumours. *Eur J Nucl Med Mol Imaging*. 2003;30:689–694.
50. Brink I, Schaefer O, Walz M, Neumann HP. Fluorine-18 DOPA PET imaging of paraganglioma syndrome. *Clin Nucl Med*. 2006;31:39–41.
51. Boedeker CC, Neumann HP, Ridder GJ, Maier W, Schipper J. Paragangliomas in patients with mutations of the SDHD gene. *Otolaryngol Head Neck Surg*. 2005; 132:467–470.
52. Hoegerle S, Althoefer C, Ghanem N, Brink I, Moser E, Nitzsche E. <sup>18</sup>F-DOPA positron emission tomography for tumour detection in patients with medullary thyroid carcinoma and elevated calcitonin levels. *Eur J Nucl Med*. 2001;28: 64–71.
53. Beuthien-Baumann B, Strumpf A, Zessin J, Bredow J, Kotzerke J. Diagnostic impact of PET with <sup>18</sup>F-FDG, <sup>18</sup>F-DOPA and 3-O-methyl-6-[<sup>18</sup>F]fluoro-DOPA in recurrent or metastatic medullary thyroid carcinoma. *Eur J Nucl Med Mol Imaging*. 2007;34:1604–1609.

54. Jacob T, Grahek D, Younsi N, et al. Positron emission tomography with [<sup>18</sup>F]FDOPA and [<sup>18</sup>F]FDG in the imaging of small cell lung carcinoma: preliminary results. *Eur J Nucl Med Mol Imaging*. 2003;30:1266–1269.
55. Dimitrakopoulou-Strauss A, Strauss LG, Burger C. Quantitative PET studies in pretreated melanoma patients: a comparison of 6-[<sup>18</sup>F]fluoro-L-dopa with <sup>18</sup>F-FDG and <sup>15</sup>O-water using compartment and noncompartment analysis. *J Nucl Med*. 2001;42:248–256.
56. Seshadri N, Wat J, Balan K. Bilateral adrenal metastases from malignant melanoma: concordant findings on <sup>18</sup>F-FDG and <sup>18</sup>F-FDOPA PET. *Eur J Nucl Med Mol Imaging*. 2006;33:854–855.
57. Lange-Nolde A, Zajic T, Slawik M, et al. PET with <sup>18</sup>F-DOPA in the imaging of parathyroid adenoma in patients with primary hyperparathyroidism: a pilot study. *Nuklearmedizin*. 2006;45:193–196.
58. Talbot JN, Kerrou K, Missoum F, et al. 6-[<sup>18</sup>F]Fluoro-L-DOPA positron emission tomography in the imaging of Merkel cell carcinoma: preliminary report of three cases with 2-deoxy-2-[<sup>18</sup>F]fluoro-D-glucose positron emission tomography or pentetretotide-(<sup>111</sup>In) SPECT data. *Mol Imaging Biol*. 2005;7:257–261.
59. Win Z, Al-Nahhas A, Rubello D, Gross MD. Somatostatin receptor PET imaging with gallium-68 labeled peptides. *Q J Nucl Med Mol Imaging*. 2007;51:244–250.
60. Wymenga ANM, Eriksson B, Salmela PI, et al. Efficacy and safety of lantreotide prolonged release in patients with gastrointestinal neuroendocrine tumors with hormone related symptoms. *J Clin Oncol*. 1999;17:1111–1117.
61. Rosch T, Lightdale CJ, Botet JF, et al. Localization of pancreatic endocrine tumors by endoscopic ultrasound. *N Engl J Med*. 1992;326:1721–1726.
62. Anderson MA, Carpenter S, Thompson NW, et al. Endoscopic ultrasound is highly accurate and directs management in patients with neuroendocrine tumors of the pancreas. *Am J Gastroenterol*. 2000;95:2271–2277.
63. Hellman P, Hennings J, Akerstrom G, Skogseid B. Endoscopic ultrasonography for evaluation of pancreatic tumours in multiple endocrine neoplasia type 1. *Br J Surg*. 2005;92:1508–1512.
64. Lenders JW, Eisenhofer G, Mannelli M, Pacak K. Pheochromocytoma. *Lancet*. 2005;366:665–675.
65. Brink I, Hoegerle S, Klisch J, Bley TA. Imaging of pheochromocytoma and paraganglioma. *Fam Cancer*. 2005;4:61–68.
66. Hoefnagel CA. Metaiodobenzylguanidine and somatostatin in oncology: role in the management of neural crest tumours. *Eur J Nucl Med*. 1994;21:561–581.
67. Ilias I, Yu J, Carrasquillo JA, et al. Superiority of 6-[<sup>18</sup>F]-fluorodopamine positron emission tomography versus [<sup>131</sup>I]-metaiodobenzylguanidine scintigraphy in the localization of metastatic pheochromocytoma. *J Clin Endocrinol Metab*. 2003;88:4083–4087.
68. Pacak K, Eisenhofer G, Carrasquillo JA, Chen CC, Li ST, Goldstein DS. [<sup>18</sup>F]Fluorodopamine positron emission tomography scanning for diagnostic localization of pheochromocytoma. *Hypertension*. 2001;36:6–8.
69. Koukouraki S, Strauss LG, Georgoulis V, Eisenhut M, Haberkorn U, Dimitrakopoulou-Strauss A. Comparison of the pharmacokinetics of <sup>68</sup>Ga-DOTATOC and [<sup>18</sup>F]FDG in patients with metastatic neuroendocrine tumours scheduled for <sup>90</sup>Y-DOTATOC therapy. *Eur J Nucl Med Mol Imaging*. 2006;33:1115–1122.
70. Ribeiro MJ, De Lonlay P, Delzescaux T, et al. Characterization of hyperinsulinism in infancy assessed with PET and <sup>18</sup>F-fluoro-L-DOPA. *J Nucl Med*. 2005;46:560–566.
71. Otonkoski T, Nanto-Salonen K, Seppanen M, et al. Noninvasive diagnosis of focal hyperinsulinism of infancy with [<sup>18</sup>F]-DOPA positron emission tomography. *Diabetes*. 2006;55:13–18.
72. de Lonlay P, Simon-Carre A, Ribeiro MJ, et al. Congenital hyperinsulinism: pancreatic [<sup>18</sup>F]fluoro-L-dihydroxyphenylalanine (DOPA) positron emission tomography and immunohistochemistry study of DOPA decarboxylase and insulin secretion. *J Clin Endocrinol Metab*. 2006;91:933–940.
73. Kauhanen S, Seppanen M, Minn H, et al. Fluorine-18-L-dihydroxyphenylalanine (<sup>18</sup>F-DOPA) positron emission tomography as a tool to localize an insulinoma or beta-cell hyperplasia in adult patients. *J Clin Endocrinol Metab*. 2007;92:1237–1244.
74. Hussain K, Seppanen M, Nanto-Salonen K, et al. The diagnosis of ectopic focal hyperinsulinism of infancy with [<sup>18</sup>F]-dopa positron emission tomography. *J Clin Endocrinol Metab*. 2006;91:2839–2842.
75. Hardy OT, Hernandez-Pampaloni M, Saffer JR, et al. Diagnosis and localization of focal congenital hyperinsulinism by <sup>18</sup>F-fluorodopa PET scan. *J Pediatr*. 2007;150:140–145.
76. Mohnike K, Blankenstein O, Christesen HT, et al. Proposal for a standardized protocol for <sup>18</sup>F-DOPA-PET (PET/CT) in congenital hyperinsulinism. *Horm Res*. 2006;66:40–42.
77. Leskinen S, Pulkki K, Knuuti J, et al. Transport of carbon-11-methionine is enhanced by insulin. *J Nucl Med*. 1997;38:1967–1970.
78. Chen W, Silverman DH, Delaloye S, et al. <sup>18</sup>F-FDOPA PET imaging of brain tumors: comparison study with <sup>18</sup>F-FDG PET and evaluation of diagnostic accuracy. *J Nucl Med*. 2006;47:904–911.



The Journal of  
NUCLEAR MEDICINE

## 6-I-<sup>18</sup>F-Fluorodihydroxyphenylalanine PET in Neuroendocrine Tumors: Basic Aspects and Emerging Clinical Applications

Pieter L. Jager, Raman Chirakal, Christopher J. Marriott, Adrienne H. Brouwers, Klaas Pieter Koopmans and Karen Y. Gulenchyn

*J Nucl Med.* 2008;49:573-586.  
Published online: March 14, 2008.  
Doi: 10.2967/jnumed.107.045708

---

This article and updated information are available at:  
<http://jnm.snmjournals.org/content/49/4/573>

---

Information about reproducing figures, tables, or other portions of this article can be found online at:  
<http://jnm.snmjournals.org/site/misc/permission.xhtml>

Information about subscriptions to JNM can be found at:  
<http://jnm.snmjournals.org/site/subscriptions/online.xhtml>

*The Journal of Nuclear Medicine* is published monthly.  
SNMMI | Society of Nuclear Medicine and Molecular Imaging  
1850 Samuel Morse Drive, Reston, VA 20190.  
(Print ISSN: 0161-5505, Online ISSN: 2159-662X)

© Copyright 2008 SNMMI; all rights reserved.